Bulgarian Journal of Physics 21 Nos 3/4 (1994) 30–40

INTERCOMPARISON OF THE EFFICIENCIES OF ROTATIONAL RAMAN AND RAYLEIGH LIDAR TECHNIQUES FOR MEASURING THE ATMOSPHERIC TEMPERATURE

I. D. IVANOVA, L. L. GURDEV, V. M. MITEV
Institute of Electronics, Bulgarian Academy of Sciences
72 Tzarigradsko shose Blvd., 1784 Sofia, Bulgaria

Received 14 July 1993

Abstract. The potential accuracies (efficiencies) of lidar techniques for measuring the atmospheric (tropospheric) temperature are compared. These techniques are based on the temperature dependence of: the envelope of the rotational Raman scattering (RRS) spectrum, the shape of the RRS spectral lines, the shape of the Rayleigh-Brillouin scattering (RBS) spectral line. The effect of the background is also taken into account. It is shown that the techniques based on Rayleigh (or Rayleigh-Brillouin) scattering are more efficient due to higher signal power and sensitivity, and more effective suppression of the background.

1. Introduction

The methods of laser remote sensing of the atmospheric temperature are based on temperature dependent parameters of interactions of light with atmospheric gases. For instance, in a number of cases the temperature dependence is used of the following: the bandwidth of resonance [1] or Rayleigh scattering [2], the envelope of the rotational Raman scattering (RRS) spectrum [3] or the shape of RRS spectral lines [4], the shape of the Rayleigh scattering (RS) or the Rayleigh-Brillouin scattering (RBS) spectrum [5] etc. The results from different investigations and applications of these methods show their feasibility and their limitations [1–11]. The various methods have various advantages and disadvantages as compared to each other but no systematic attempt has been undertaken so far (except for [5, 11]) to compare their potential accuracies as principal characteristics of their potential efficiencies. Two RRS techniques for remote sensing of the atmospheric temperature [3, 4] have been recently compared in the above sense [11] supposing identical experimental conditions, e. g. laser source, receiving optics, noise, atmospheric conditions etc. The first of the compared RRS techniques [3] is based on the temperature dependence of the

 ©1995 St. Kliment Ohridski University Press All rights reserved

RRS spectrum envelope. The second one is based on the use of Fabry-Perot interferometer as a comb filter for analysis of the temperature-dependent RRS spectrum shape.

The RRS methods have been developed most considerably, and have provided the most reliable results for the troposphere [3, 4, 6–8] and the lower stratosphere. At the same time, the methods making use of the RS bandwidth [9, 10] or based on high-resolution analysis of the RBS line [5] seem to be very promising ones. That is why the purpose of the present work is to compare the efficiencies of the RRS and the RS (RBS) methods.

2. Principal Parameters of the Considered Methods

2.1. Rotational Raman scattering methods

For monochromatic incident light with frequency ω_0, the RRS spectrum of some simple linear molecule gas component K consists of Stokes (S-branch) lines with frequencies $\omega_{J,K} = \omega^S_{J,K} = \omega_0 - 4B_{0,K}\left(J + \frac{3}{2}\right)$ due to the transitions $J \to J+2$, and anti-Stokes (O-branch) lines with frequencies $\omega_{J,K} = \omega^S_{J,K} = \omega_0 + 4B_{0,K}\left(J - \frac{1}{2}\right)$ due to the transitions $J \to J-2$. Above, $B_{0,K}$ is the rotational constant, and J is the rotational quantum number. The corresponding backscattering cross sections are $\sigma_{J,K} = \frac{64\pi^4}{45} b_{J,K}\gamma_K^2\omega_{J,K}^4$, where $b_{J,K}$ is the Placzek-Teller coefficient for the S- or O-branches, and γ_K^2 is the anisotropy of the molecular polarizability tensor (in more detail, see [12]). The lidar equation for a single RRS line can be written in the form:

$$P_{J,K}(T) = \frac{1}{z^2} P_i A_0 L \tau_0(z)\eta(z) N_K \sigma_{J,K} F_{J,K}(T)\tau_{J,K}(z) \qquad (1)$$

where $P_{J,K}(T)$ is the received backscattered power, P_i is the incident light (laser) power, A_0 is the lidar constant, L is the length of the scattering volume, $\eta(z)$ is the receiving efficiency of the lidar, N_K is the number density of molecules. The atmospheric transmittances at frequencies ω_0 and $\omega_{J,K}$ along the z-long light propagation path to the scattering volume are denoted $\tau_0(z)$ and $\tau_{J,K}(z)$ respectively. Further we suppose that $\tau_0(z) \approx \tau_{J,K}(z)$. The fraction $F_{J,K}(T)$ of molecules K in initial state J, at absolute temperature T is given by [12]

$$F_{J,K}(T) = \frac{1}{Q} g_{J,K}(2J+1)\exp\left(-\frac{E_J}{kT}\right) \qquad (2)$$

where $Q \approx (2I_K+1)^2 \frac{kT}{2hcB_{0,K}}$ is the rotational partition function, I_K is the nuclear-spin quantum number, $E_J \approx J(J+1)hcB_{0,K}$ is the rotational energy, $g_{J,K}$ is the statistical weight factor, h is the Plank constant, k is the Boltzmann constant, c is the light velocity.

The RRS power from air ($N_2 + O_2$), integrated by an optical filter with spectral response function $\Gamma_q(\omega_J)$ centered at frequency ω_q ($q = 1, 2$), can be written in the form:

$$P_q = \sum_{K,J} \Gamma_q(\omega_J) P_{K,J}(T) .$$

A property of the integrated RRS spectrum is that there are wavelength intervals $\delta = (\lambda_0 \pm \Delta\lambda_{10}, \lambda_0 \pm \Delta\lambda_{20})$ around the exciting wavelength $\lambda_0 = \dfrac{2\pi c}{\omega_0}$, such that for every central wavelength $\lambda_q = \dfrac{2\pi c}{\omega_q} = \lambda_1 \in \delta$ the corresponding power $P_q = P_1$ is a decreasing function of T. And on the contrary, for $\lambda_q = \lambda_2 \notin \delta$, $P_q = P_2$ is an increasing function of T [7]. The idea of the RRS spectrum envelope methods [6, 8] is as follows: combining P_1 and P_2 to compose some unambiguous functions $\phi(T) = R(P_1, P_2)$ which allow us to determine T by measuring P_1 and P_2. The combination usually used is simply the ratio $R = \dfrac{P_1}{P_2}$.

In the interferometric method, the scanning Fabry-Perot interferometer (FPI) is used as a comb filter for processing the periodic RRS spectrum of nitrogen [4]. In this case, the total transmitted Raman power (or energy $E_n = P_n T_i$ integrated over a measuring period T_i) at the n-th order interferogram maximum can be expressed [4] by

$$P_n = P(\Delta_n) = \sum_{J=0}^{\infty} \left[P_{J,S} \int \Phi(x + \alpha_{J,n}) T(x) dx + P_{J+2,O} \int \Phi(x + \beta_{J,n}) T(x) dx \right] \tag{3}$$

where

$$\alpha_{J,n} = \Delta_0 \left[\frac{(J+2)(n+\varepsilon_n)}{m_0 + n} - \varepsilon_n \right]$$

$$\beta_{J,n} = -\Delta_0 \left[\frac{(J+1)(n+\varepsilon_n)}{m_0 + n} + \varepsilon_n \right] .$$

Δ_n is the free spectral range that gives the peak Raman transmittance in the n-th order of the interferogram, $\Delta_0 = 4B_0$ is the free spectral range at the matched condition, m_0 is a reference order ($m_0\Delta_0 = \omega_0 + \Delta_0/2$), ε_n is a parameter which is determined numerically. The transmittance of the FPI is

$$T(x) = \frac{\dfrac{\pi \Delta\omega_F}{2} \dfrac{\Delta\omega_F}{2\pi}}{x^2 + \left(\dfrac{\Delta\omega_F}{2} \right)^2}$$

where $\Delta\omega_F = \dfrac{\Delta}{F}$ is the instrumental width, Δ is the free spectral range, and F is the finesse of the interferometer. The RRS line in the troposphere is assumed to have Lorentzian shape

$$\Phi(\omega) = \frac{\dfrac{\Delta\omega}{2\pi}}{\omega^2 + \left(\dfrac{\Delta\omega}{2}\right)^2}$$

with half-maximum width (in cm^{-1}) $\Delta\omega = 0.5\sigma^2 p(M_w T)^{-\frac{1}{2}}$, where p is the pressure in atmospheres, M_w is the molecular weight, σ is the optical collision diameter in Å. For nitrogen, $\Delta\omega = \dfrac{1.59p}{\sqrt{T}}$ (cm^{-1}).

Eq. (4) is obtained assuming that each RRS line cannot be transmitted by more than a single order of the FPI. Besides, as far as we consider here only RRS from N_2, we have replaced in (3) the subscript K by the subscripts S and O in order to denote the Stokes and anti-Stokes lines, respectively.

Due to the temperature and the pressure dependence of the RRS linewidth $\Delta\omega$, the Fabry-Perot interferogram maxima $P(\Delta_n)$ are also functions (unambiguous) of the temperature and the pressure.

2.2. Rayleigh (Rayleigh-Brillouin) scattering methods

RS spectrum from the atmosphere is Doppler broadened due to the thermal motion of the molecules. Therefore the spectral shape and the linewidth depend on the temperature and these dependences can be used for measuring atmospheric temperature. In order to simplify the evaluation of the measurement error we assume, following [9], Doppler form of the RS (RBS) spectrum:

$$I(\omega) = P_0(\pi\gamma^2)^{-\frac{1}{2}} \exp\left[-\frac{(\omega-\omega_0)^2}{\gamma^2}\right] \tag{4}$$

where P_0 is input RS power, $\gamma = \dfrac{2\omega_0}{c}\sqrt{bT}$, and $b = 5.74 \times 10^2\,\mathrm{m^2 s^{-2} K^{-1}}$ is a constant in the troposphere. The lidar equation for P_0 is

$$P_0 = \frac{1}{z^2} P_i A_0 L \tau_0^2(z)\eta(z) N_K \sigma_{RS}\,, \tag{5}$$

where σ_{RS} is RS differential cross section.

The first considered here RS method based on temperature dependence of RS linewidth employs two Michelson interferometers (MI) in parallel [9]. The outputs P_q ($q = 1, 2$) of the interferometers, at optical path differences $2d_q$ between the delayed and undelayed signal parts, are given by

$$P_q = \frac{P_0}{4}\left[1 - \exp(-d_q^2 M)\right] \tag{6}$$

when d_q correspond to some minima of the oscillatory factors of the output. Then $d_q = \frac{k_q c\pi}{\omega}$, where k_q are odd numbers. In [8], $M = \frac{\gamma^2}{c^2}$. The ratio $R = \frac{P_1}{P_2}$ is an unambiguous function $R = f(T)$. The inverse function $T = f^{-1}(R)$ allows to determine T. As shown in [9], if a Gaussian-shaped prefilter is used with transmittance bandwidth equal to 4γ, the background spectral density can be considered as a constant. The aerosol-backscattering noise is practically rejected.

The method based on high-resolution analysis of RS (RBS) spectral shape [5] employs two narrow-band absorbing block filters with absorption bandwidths γ_q $(q = 1, 2)$ such that $\gamma_1 \ll \gamma_2$. The corresponding spectral transmittance functions are $B_q(\omega)$. The block filters are used to suppress the aerosol backscatter and to form two portions of RBS power

$$P_q^b = \int B_q(\omega) I(\omega) d\omega \ . \tag{7}$$

The first portion includes approximately the whole RBS spectrum power. The second portion includes only a wing part of it. We consider the ratio $R(T) = \frac{P_w}{P_c}$ as providing temperature information where $P_w = P_2^b$ is the wing part and $P_c = P_1^b - P_2^b$ is the central part of the RS line power.

3. Comparison of the Efficiencies

The efficiency of the compared methods characterizes the possibility to measure the atmospheric temperature in a fast and accurate way. The potential efficiency of the methods is considered as depending mainly on their physical nature. In this case it is supposed that the necessary requirements to the experimental setup are satisfied. Besides, it is supposed that there are some optimal relations with respect to the efficiency between the parameters of the setup, which are also satisfied. The root-mean-square error σ in the measurement of the atmospheric temperature which is estimated under the above-mentioned conditions is a quantitative measure of the potential efficiency. However, we have chosen the reciprocal value $\varepsilon = \sigma^{-1}$ (the potential accuracy) as a more appropriate characteristic proportional to the efficiency. As it is seen below, the larger σ^{-1} the less the time which is necessary to achieve a prescribed accuracy.

All methods described in Sec. 2 are based on the unambiguous temperature dependence of a ratio $R = f(T) = P_1/P_2$ of the signal powers P_1 and P_2 measured in two lidar channels. Then the temperature is determined by the inverse functions $T = f^{-1}(R = P_1/P_2)$. Since the powers P_1 and P_2 are very feeble they are usually measured in photon counting mode of detection. In this case, the measured quantities in both lidar channels are the corresponding total mean numbers of photocounts $Q_{1,t} = Q_1 + Q_{1,N}$ and $Q_{2,t} = Q_2 + Q_{2,N}$, accumulated in some measuring time interval t_m. The values of $Q_1 = \alpha P_1 t_m$ and $Q_2 = \alpha P_2 t_m$ correspond to the signal powers P_1 and P_2; α is the photodetector quantum efficiency. The values of $Q_{1,N} = \alpha P_{1,N} t_m + Q_{1,D}$ and $Q_{2,N} = \alpha P_{2,N} t_m + Q_{2,D}$ correspond to the background

powers $P_{1,N}$ and $P_{2,N}$ and include the dark counts $(Q_{1,D}, Q_{2,D})$. The expression of the ratio R acquires the form $R = Q_1/Q_2$. Because of the background, the dark counts and the statistical fluctuations, the values of Q_1 and Q_2 are always determined with some errors dQ_1 and dQ_2 respectively. This leads to an error dT in the determination of the temperature T. At sufficiently small values of dQ_1 and dQ_2 we may formally write

$$dT = \left(\frac{dR}{dT}\right)^{-1} \left[\frac{\partial R}{\partial Q_1} dQ_1 + \frac{\partial R}{\partial Q_2} dQ_2\right] . \tag{8}$$

From there it follows that

$$\sigma = \langle (dT)^2 \rangle^{\frac{1}{2}} = \left(\frac{\partial \ln R}{\partial T}\right)^{-1} \left[\frac{DQ_1}{Q_1^2} + \frac{DQ_2}{Q_2^2}\right]^{\frac{1}{2}} . \tag{9}$$

In Eq. (9) the values $DQ_1 = \langle (dQ_1)^2 \rangle$ and $DQ_2 = \langle (dQ_2)^2 \rangle$ are the variances of the errors dQ_1 and dQ_2 respectively; $\langle . \rangle$ denotes ensemble average. It is also supposed that the errors dQ_1 and dQ_2 are uncorrelated statistically. The statistical estimates $\hat{Q}_1$ and $\hat{Q}_2$ (respectively of Q_1 and Q_2) are usually obtained by subtraction of the noise, i.e. $\hat{Q}_1 = \hat{Q}_{1,t} - \hat{Q}_{1,N}$ and $\hat{Q}_2 = \hat{Q}_{2,t} - \hat{Q}_{2,N}$ where $\hat{Q}_i$ is the estimate of Q_i. Then we have $D\hat{Q}_1 = D\hat{Q}_{1,t} + D\hat{Q}_{1,N}$ and $D\hat{Q}_2 = D\hat{Q}_{2,t} + D\hat{Q}_{2,N}$ where $D\hat{Q}_i$ is the variance of the corresponding estimate $\hat{Q}_i$. As far as the photocounts have Poissonian statistics, we can write that

$$D\hat{Q}_1 = \frac{Q_1 + 2Q_{1,N}}{M} \qquad D\hat{Q}_2 = \frac{Q_2 + 2Q_{2,N}}{M} \tag{10}$$

where M is the number of measurements (proportional to the whole measuring time) to store statistical data. So we see that $DQ_{1,2} \to 0$ when $M \to \infty$, i.e. Eq. (8) is asymptotically exact on the average. By replacing expressions of Eq. (10) in Eq. (9) we obtain the following estimate $\hat{\sigma}$ of the root-mean-square error:

$$\hat{\sigma} = \frac{1}{\sqrt{M}} \left(\frac{d \ln R}{dT}\right)^{-1} \left[\frac{Q_1 + 2Q_{1,N}}{Q_1^2} + \frac{Q_2 + 2Q_{2,N}}{Q_2^2}\right]^{\frac{1}{2}} . \tag{11}$$

Eq. (11) shows that $\hat{\sigma} \to 0$ when $M \to \infty$. Consequently, the estimate $\hat{T} = f^{-1}\left(\hat{Q}_1/\hat{Q}_2\right)$ of the temperature is asymptotically unbiased and consistent one. Let us write Eq. (11) as $\hat{\sigma} = \frac{\sigma}{\sqrt{M}}$ and interpret σ as an error estimate at one only measurement. Obviously, the less σ (the larger $\varepsilon = \sigma^{-1}$) the less the measuring time ($\sim M$) to achieve a prescribed acceptable error $\hat{\sigma}$.

Let us further introduce designations of the potential accuracies $\varepsilon_{\mathrm{ENV}} = \sigma_{\mathrm{ENV}}^{-1}$, $\varepsilon_{\mathrm{FPI}} = \sigma_{\mathrm{FPI}}^{-1}$, $\varepsilon_{\mathrm{MI}} = \sigma_{\mathrm{MI}}^{-1}$, and $\varepsilon_{\mathrm{HR}} = \sigma_{\mathrm{HR}}^{-1}$, corresponding to the RRS envelope method, to the RRS interferometric method, to the RS interferometric method, and to the RS high resolution method. It is convenient to chose e. g. $\varepsilon_{\mathrm{ENV}}$ as a reference quantity and to compare the ratios $\chi_0 = \frac{\varepsilon_{\mathrm{ENV}}}{\varepsilon_{\mathrm{ENV}}} = 1$, $\chi_1 = \frac{\varepsilon_{\mathrm{FPI}}}{\varepsilon_{\mathrm{ENV}}}$, $\chi_2 = \frac{\varepsilon_{\mathrm{MI}}}{\varepsilon_{\mathrm{ENV}}}$, and

$\chi_3 = \frac{\varepsilon_{HR}}{\varepsilon_{ENV}}$ which may be interpreted as relative (with respect to ε_{ENV}) efficiencies. Evidently, a method "i" is more efficient than a method "j" always when $\chi_i > \chi_j$.

Certainly, we should assume identical experimental conditions such as power and wavelength of the exciting radiation, state of the atmosphere, transmittance of the receiving optics, noise level etc. In this case, such values as P_0, $\tau_0(z) = \tau_{J,K}(z)$, A_0, $\eta(z)$, N_K, and z (See Eqs (1) and (5)) are reduced. Therefore, they are not specified. The other characterizing parameters for all methods are chosen in an optimal way so that the corresponding root-mean-square errors σ_{ENV}, σ_{FPI}, σ_{MI}, and σ_{HR} to have minimum values in absence of background (when $Q_{1,N} = 0$ and $Q_{2,N} = 0$). The errors are estimated by use of Eq. (11).

The error σ_{ENV} is estimated on the basis of relations and parameters described in Sec. 2. All necessary molecular constants are taken from [11] where only the value of γ_K^2 may be a subject of discussion. The parameters to be optimized here are the central wavelengths λ_q and the spectral width $\Delta\lambda_G$ of the optical filter spectral response function $G_q(\omega) = \exp\left[-(\omega - \omega_q)^2/(\Delta\omega_G)^2\right]$ assumed to be a Gaussian one. The optimum is an compromise between the increase of the sensitivity and the simultaneous decrease of the signal power e. g. when narrowing the spectral response function. Here and everywhere below the optimization is performed numerically by varying widely the parameters of interest and the temperature. As a result we have obtained that at an exciting wavelength $\lambda_0 = \frac{2\pi c}{\omega_0} = 510.6\,\text{nm}$ and temperatures from 220 K to 320 K the optimal parameters are $\lambda_1 = 510.9\,\text{nm}$, $\lambda_2 = 514.8\,\text{nm}$, and $\Delta\lambda_G = \frac{2\pi c \Delta\omega_G}{\omega_q^2} = 10\,\text{Å}$.

For the RRS interferometric method $P_1 = P(\Delta_n)$ and $P_2 = P(\Delta_0)$. The parameters to be optimised are interferogram order n and the finesse F. As above the optimum is a result of the balance between the sensitivity increase and the signal power decrease. For pressures from 0.6 atm to 1 atm and temperatures from 220 K to 320 K the optimal parameters are $n = 5$ and $F = 70$. The band of the RRS spectral lines with essential contribution to the interferogram is supposed to be $210\,\text{cm}^{-1}$ wide beginning from ω_0. The comparison is performed at fixed pressure $p = 1\,\text{atm}$.

For the RS interferometric method we have varied the parameters d_1 and d_2. At temperatures from 220 K to 320 K an optimal pair is $d_1 = 3.28\,\text{cm}$ and $d_2 = 6.56\,\text{cm}$.

For the RS high resolution method $P_1 = P_c$ and $P_2 = P_w$. To simplify the analysis and the calculations, as well as to test the influence on the results of the shape of the transmittance functions $B_q(\omega)$ we make use of the following approximations:

$$B_q(\omega) = 1 - \exp\left[-\frac{(\omega - \omega)0)^2}{\gamma_q^2}\right]. \tag{12}$$

and

$$B_q(\omega) = \begin{cases} 0 & \text{for } |\omega - \omega_0| \leq \gamma_q \\ 1 & \text{for } |\omega - \omega_0| > \gamma_q \end{cases} \tag{13}$$

On the basis of Eqs (4), (7) and (12) for the first approximation we obtain

$$P_q^b = \frac{P_0}{2}\left[1 - \frac{\gamma_q}{\sqrt{\gamma^2 + \gamma_q^2}}\right] . \tag{14}$$

For the second approximation, from Eqs (4), (7) and (13) we obtain

$$P_c = \frac{P_0}{2}\Phi\left(\frac{\gamma_q}{\gamma}\right) , \qquad P_w = \frac{P_0}{2}\left[1 - \Phi\left(\frac{\gamma_q}{\gamma}\right)\right] . \tag{15}$$

where the error function $\Phi(x)$ is taken from tables. Comparing the asymptotic-series expansion for the smooth (Gaussian) and the sharp (rectangular) transmittance functions of the block filter we see that the behaviour of R does not depend essentially on the type of the transmittance function. Consequently, the result from the comparison performed here should not depend essentially on the choice of the transmittance function. This fact is illustrated in Figs 3*a* and 3*b*. The use of a Gaussian-shaped prefilter with bandwidth equal to 4γ is also supposed. The background is assumed to have a constant spectral density within the prefilter spectral band.

The parameters to be optimized here are γ_1 and γ_2. They should be chosen so that at the temperatures of interest σ_{HR} to have a minimum because of sufficiently powerful signal and high sensitivity. The estimations show that the optimal values are $\gamma_1 \to 0$ and $\gamma_2 \approx \gamma$.

The noise is considered as an effective background specified by its spectral density. The latter is determined in relative units with respect to the spectral density at the peak of the most intensive RRS line ($J = 8$), at temperature $T = 273$ K and pressure $p = 1$ atm.

The calculated ratios χ_1, χ_2 and χ_3 vs T are shown in Figs 1, 2 and 3 (*a* and *b*) respectively, for different background levels l in the above sense: $l = 10, 5, 2, 1, 0.5, 0.1$. The analysis of the results shows that at low noise levels ($l = 0.1$) we have $1 \leq \chi_1 \ll \chi_2 \approx \chi_3$. So, the relation between the selected signal powers and the sensitivities of the different methods determine a considerably higher efficiency of the RS (RBS) methods. The main reason for this is the lower signal power of the RRS methods. In this case, the RS methods have comparable efficiencies. Comparable are also the efficiencies illustrated in Figs 3*a* and 3*b* which correspond to a smooth (Gaussian) and a sharp (rectangular) block filter transmittance function. The RRS methods also have comparable efficiencies. The increase of the noise level leads to an increase of χ_1, χ_2, and χ_3 so that $1 \ll \chi_1 \ll \chi_2 \approx \chi_3$. Consequently, the RRS methods are more sensitive to noise due to the lower signal power. RS methods have again comparable efficiencies. At the same time, the FPI method exceeds the envelope method due to the lower noise penetration. With the increase of the noise level the ratios χ_1, χ_2, and χ_3 tend to some upper limits determined by the signal powers, the sensitivities and the noise admittances.

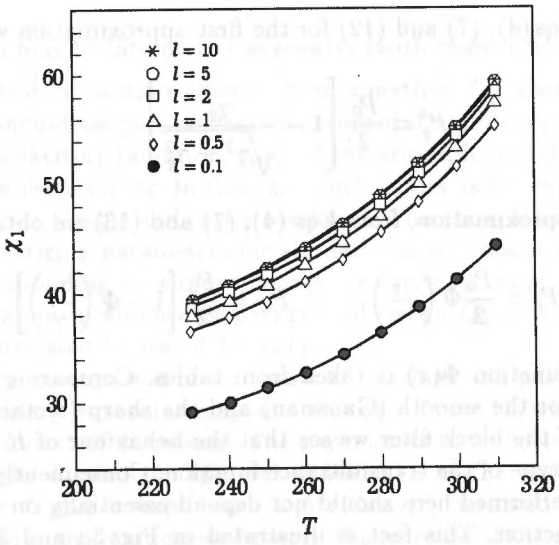

Fig. 1. Relative efficiency $\chi_1 = \frac{\varepsilon_{FPI}}{\varepsilon_{ENV}}$ of the RRS interferometric method as a function of the absolute temperature T at different noise levels l. The curves $l = 5$ and $l = 10$ coincide

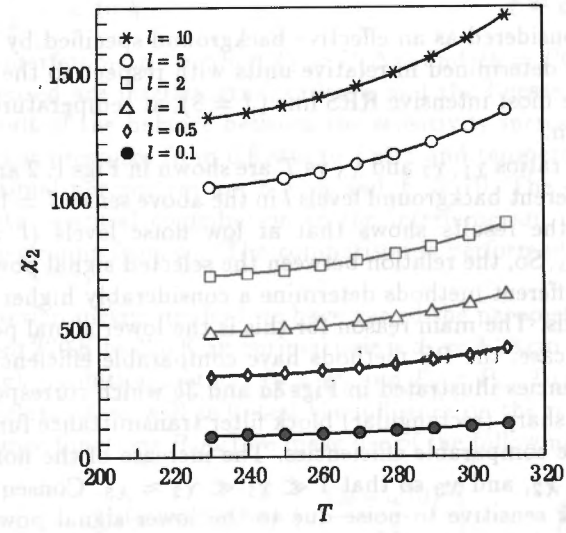

Fig. 2. Relative efficiency $\chi_2 = \frac{\varepsilon_{MI}}{\varepsilon_{ENV}}$ of the RS interferometric method as a function of the absolute temperature T at different noise levels l

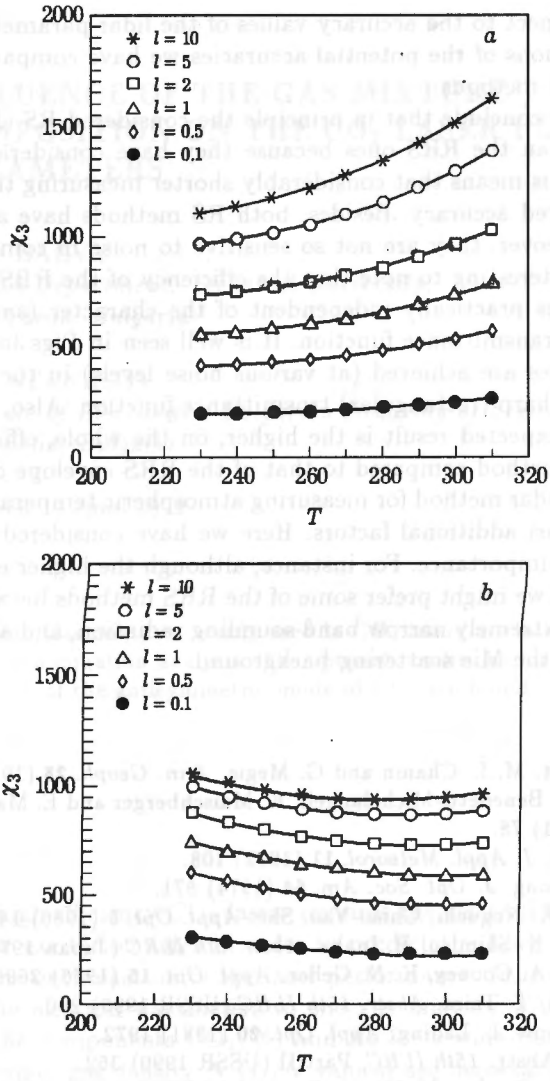

Fig. 3. Relative efficiency $\chi_3 = \frac{\varepsilon_{HR}}{\varepsilon_{ENV}}$ of the RBS high spectral resolution method as a function of the absolute temperature T at different noise levels l and a smooth (a) and a sharp (b) block filter transmittance functions

4. Conclusion

In the present work we have derived and analysed expressions for the potential accuracies of two RRS methods and two RS (RBS) methods of measuring the atmospheric temperature. On the basis of this expressions we have found some

optimal with respect to the accuracy values of the lidar parameters. By use of the obtained expressions of the potential accuracies we have compared the efficiencies of the considered methods.

Thus, we may conclude that in principle the considered RS (RBS) methods are more efficient than the RRS ones because they have considerably higher potential accuracy. This means that considerably shorter measuring time intervals allow to reach a required accuracy. Besides, both RS methods have always comparable efficiencies. Moreover, they are not so sensitive to noise in comparison with RRS methods. It is interesting to note that the efficiency of the RBS high spectral resolution method is practically independent of the character (smooth or sharp) of the block filter transmittance function. It is well seen in Figs 3*a* and 3*b* that comparable efficiencies are achieved (at various noise levels) in the case of a smooth (Gaussian) and sharp (rectangular) trnsmittance function. Also, an interesting and to some extent expected result is the higher, on the whole, efficiency of the RRS interferometric method compared to that of the RRS envelope one. Certainly, the final choice of a lidar method for measuring atmospheric temperature profiles might depend on various additional factors. Here we have considered only one of them having principal importance. For instance, although the higher efficiency of the RS (RBS) methods, we might prefer some of the RRS methods because the latter ones do not require extremely narrow band sounding radiation, and allow to avoid easier the influence of the Mie scattering background.

References

1. J. E. Blamont, M. L. Chanin and G. Megie. *Ann. Geoph.* **28** (1972) 833.
2. G. Fiocco, G. Benedetti-Michelangeli, K. Maischberger and E. Madonna. *Natur. Phys. Sci.* **229** (1971) 78.
3. J. A. Cooney. *J. Appl. Meteorol.* 11 (1972) 108.
4. R. L. Armstrong. *J. Opt. Soc. Am.* **64** (1974) 871.
5. H. Shimisu, K. Noguchi, Chiao-Yao. She. *Appl. Opt.* **5** (1986) 1460.
6. T. Kobayasi, H. Shimisu, H. Inaba. *Abstr. 6th ILRC* (Japan 1974) 49.
7. A. Cohen, J. A. Cooney, K. N. Geller. *Appl. Opt.* **15** (1976) 2696.
8. T. Kobayashi, T. Taira. *Abstr. 15th ILRC* (USSR 1990) 290.
9. R. L. Schwiesow, L. Lading. *Appl. Opt.* **20** (1981) 1972.
10. W. Shmidt. Abstr. *15th ILRC*, Part II (USSR 1990) 362.
11. L. Ivanova, L. Gurdev, V. Mitev. *Proc. of IGARSS*, Espoo (Finland 1991) 923.
12. C. M. Penney, R. L. St. Peters, M. Lapp. *J. Opt. Soc. Am.* **64** (1974) 712.